Nano-delivery systems for photothermal/starvation therapy and enhanced ferroptosis-immunotherapy

*Lanfu Zheng[1], Wei Jiang[2], * Shuming Tian[1], Zepeng Feng[1], Yanan Qi[1], Hongyang Fu[1], Liting Qi[1], Lianrui Chen[1]*

[1]Jiamusi University, Jiamusi 154007, China

[2]The First Affiliated Hospital of Jiamusi University, Jiamusi 154007, China

*Corresponding author at: The First Affiliated Hospital of Jiamusi University, No. 348 Dexiang Street, Jiamusi 154007, P.R. China

Tel +86-13704547007; Email address: 11096057@qq.com.

Supporting Information

Supporting figures

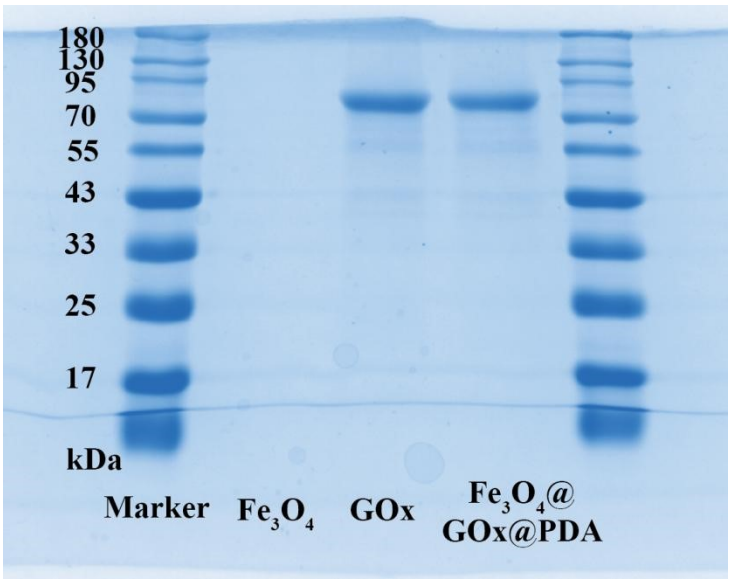

Figure S1 SDS-PAGE gel electrophoresis images of Fe_3O_4, GOx, and Fe_3O_4@GOx@PDA.

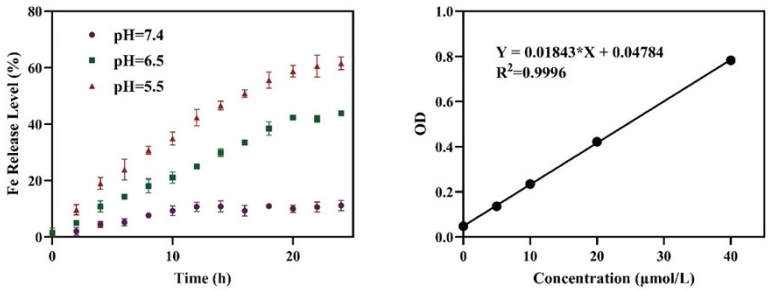

Figure S2 Fe release levels of Fe_3O_4@GOx@PDA over 24 hours in buffer solutions at pH=7.4, 6.5, and 5.5. Data represent mean ± SD, n = 3.

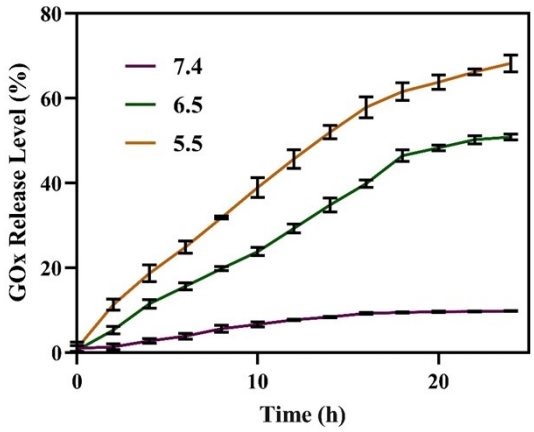

Figure S3 GOx release levels of Fe_3O_4@GOx@PDA over 24 hours in buffer solutions at pH=7.4, 6.5, and 5.5. Data represent mean ± SD, n = 3.

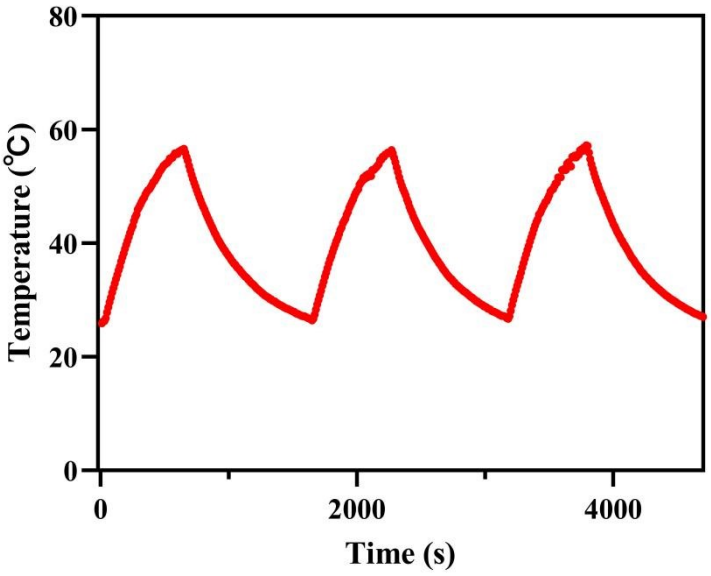

Figure S4 Temperature curve of Fe_3O_4@GOx@PDA after three heating-cooling cycles.

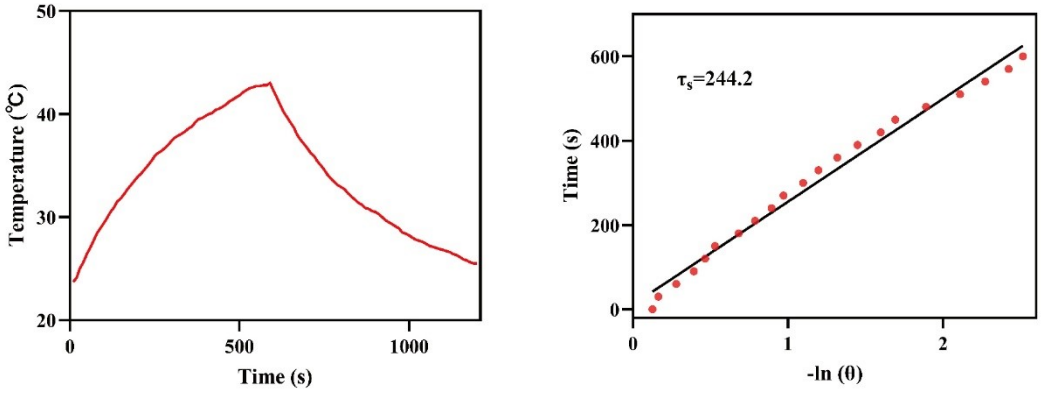

Figure S5 Temperature profiles of Fe_3O_4@GOx@PDA with time and linear profiles of -Ln(θ) with time during the cooling period.

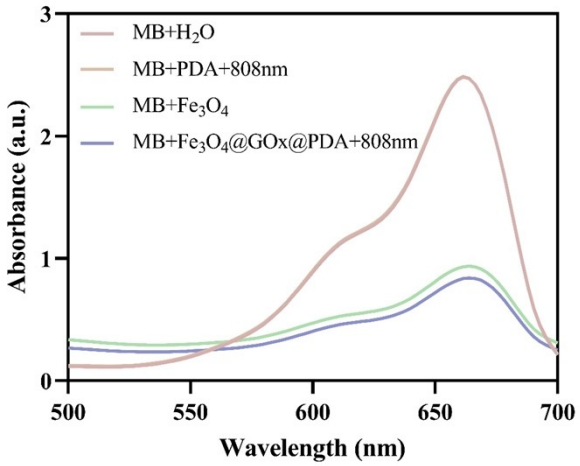

Figure S6 MB detection of H_2O, PDA+808 nm, Fe_3O_4, and Fe_3O_4@GOx@PDA+808 nm group ·OH generation.

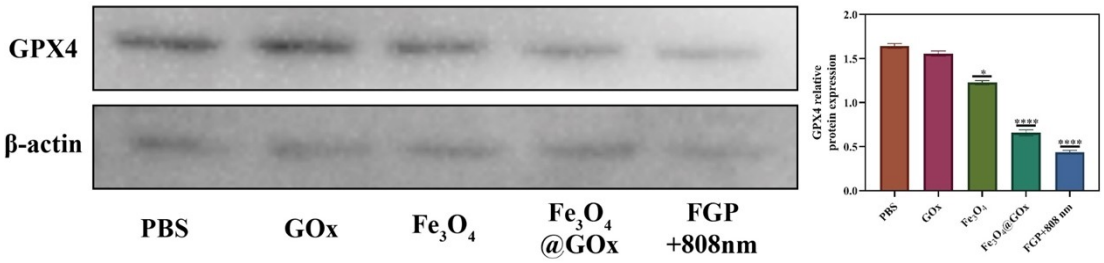

Figure S7 Western blot analysis was performed to detect and quantify GPX4 protein expression in CT26 cells following treatment with different nanomedicines. Data represent mean ± SD (n = 3; *p < 0.05, ***p < 0.001, ****p < 0.0001).

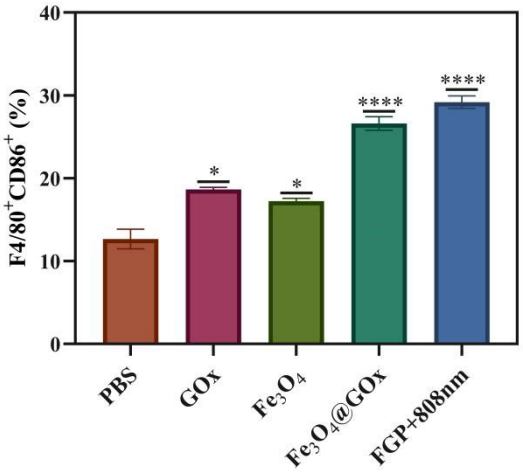

Figure S8 Flow cytometry quantification of M1 macrophage proportion. Data represent mean ± SD (n = 3; *p < 0.05, ****p < 0.0001).

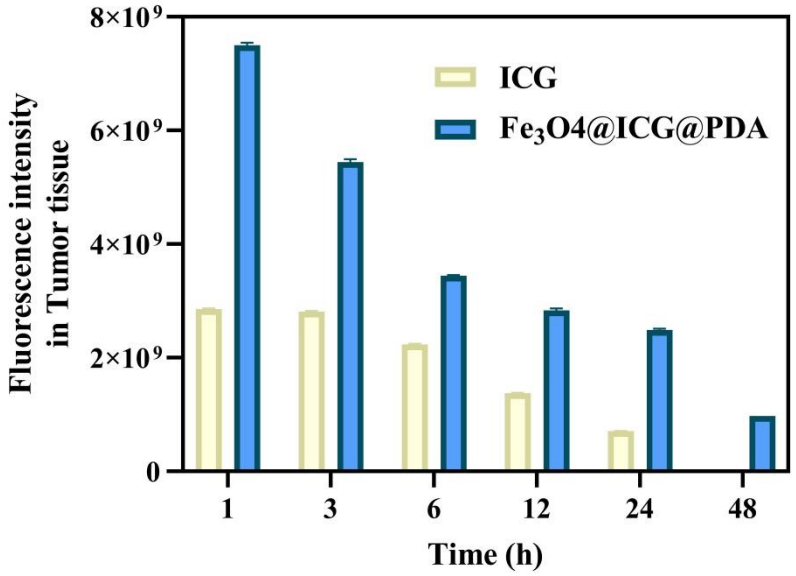

Figure S9 Quantification of fluorescence intensity at tumor sites in mice. Data represent mean ± SD, n = 3.

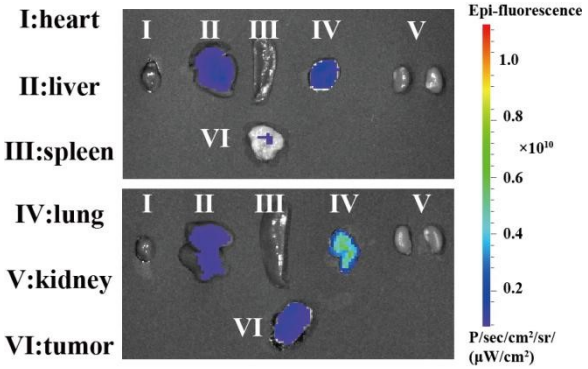

Figure S10 Distribution of Fe_3O_4@ICG@PDA in organs.

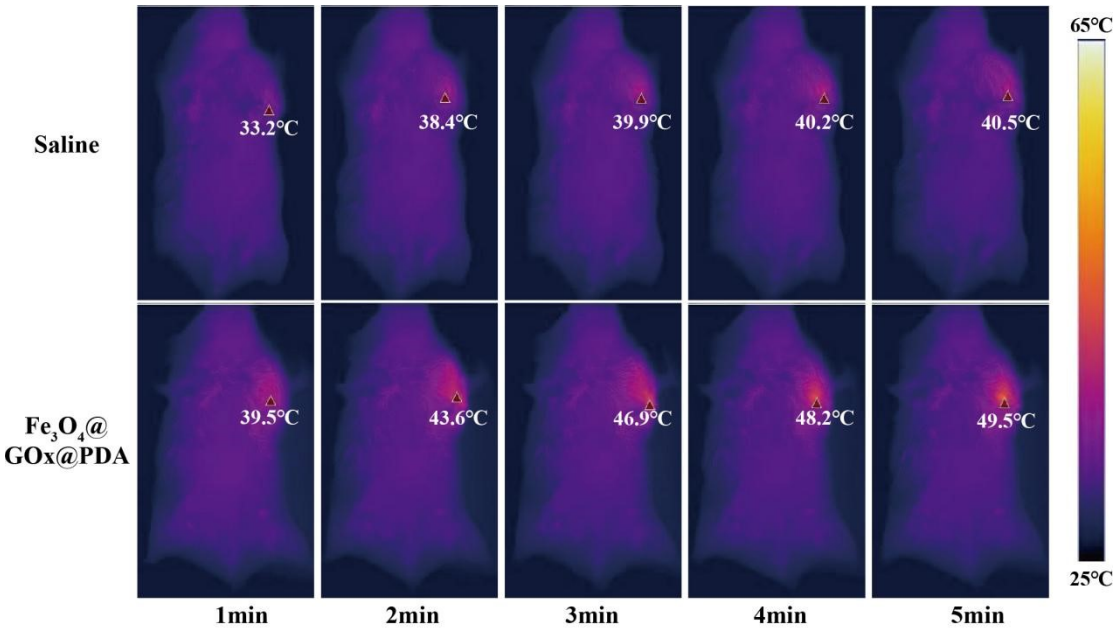

Figure S11 Photothermal imaging in mice.

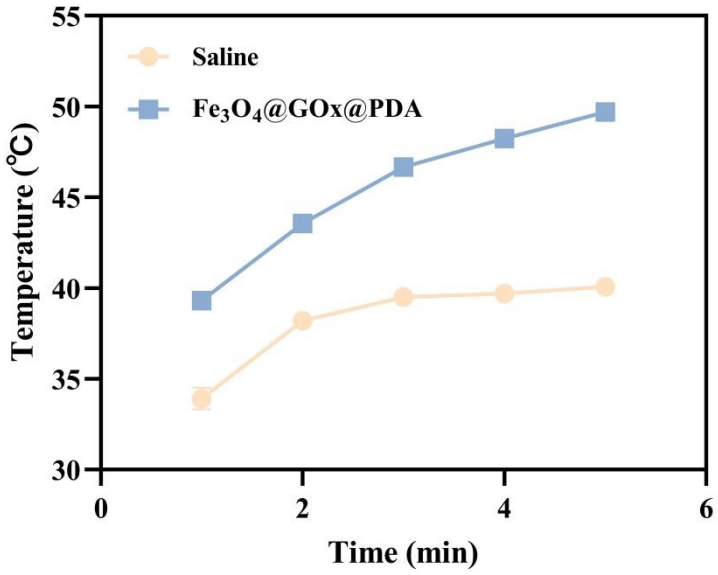

Figure S12 Quantification of photothermal temperature at tumor sites in mice. Data represent mean ± SD, n = 3.

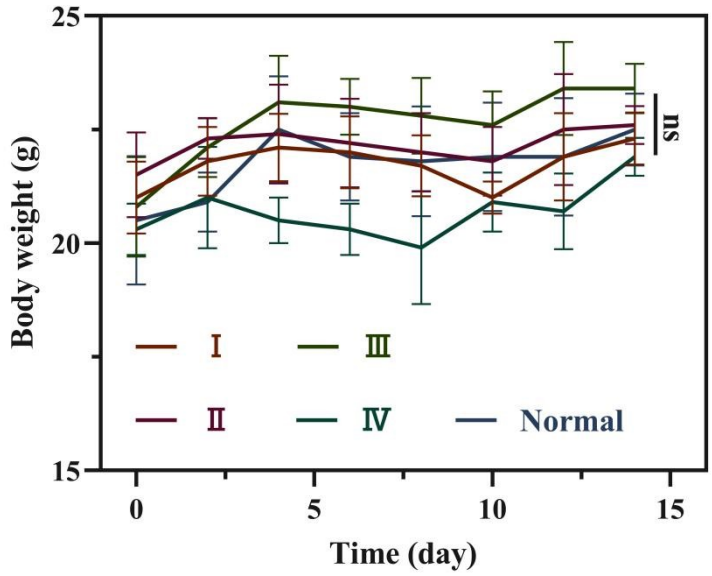

Figure S13 Trend chart of body weight changes in mice after treatment in different groups (I: Saline; (II) GOx, (III) Fe_3O_4@GOx, and (IV) Fe_3O_4@GOx@PDA + 808 nm laser). Data represent the mean ± SD (n = 4, ns: not significant).

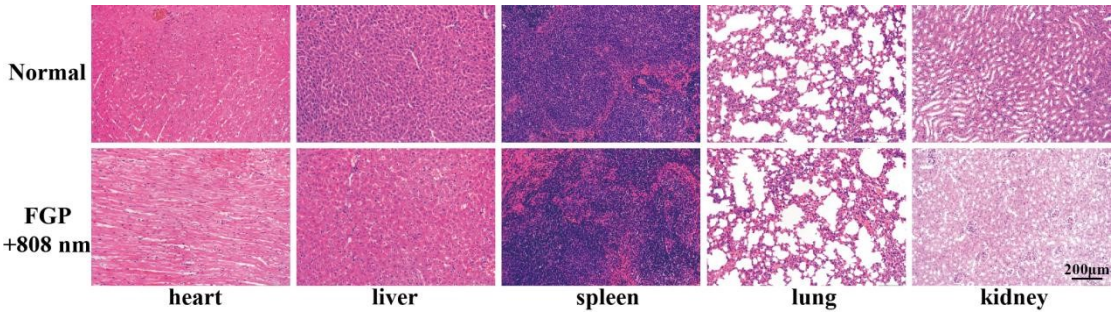

Figure S14 H&E staining results of major organs (heart, liver, spleen, lung, kidney) in mice from the control group and the FGP+808 nm treatment group.

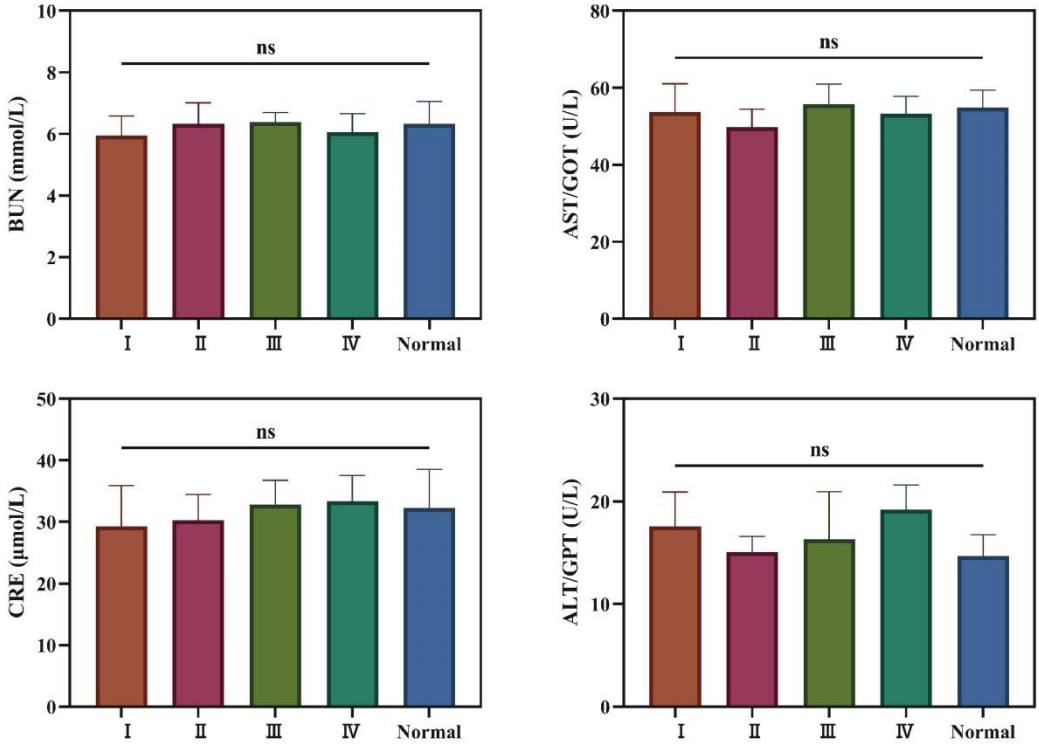

Figure S15 BUN, AST, CRE, and ALT levels were measured in mouse serum (I: Saline; (II) GOx, (III) Fe_3O_4@GOx, and (IV) Fe_3O_4@GOx@PDA + 808 nm laser). Data represent the mean ± SD(n = 4, ns: not significant).

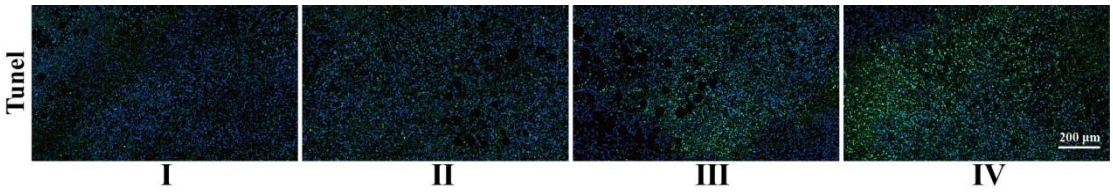

Figure S16 Representative images of Tunel staining in tumor tissue sections from different groups (I: Saline; (II) GOx, (III) Fe_3O_4@GOx, and (IV) Fe_3O_4@GOx@PDA + 808 nm laser).